

Invariant Nonlinear Correlations via Fourier Transform

Ángel Coronel-Beltrán¹ and Josué Álvarez-Borrego²

¹*Universidad de Sonora, Departamento de Investigación en Física,*

²*CICESE, División de Física Aplicada, Departamento de Óptica,
México*

1. Introduction

A great advance has been done in optical and digital pattern recognition since the first introduction of the well known classical matched filter (CMF) (Vander Lugt, 1964), which was the cornerstone for the developments of new and more effective filters. However, the use of the CMF is inefficient because the output correlation peak is degraded drastically by the geometrical distortions of the target, such as scale and rotation changes. Many attempts have been done to achieve distortion-invariant sensitivity pattern recognition. To overcome these problems, the Fourier-Mellin transform was introduced (Casasent, 1976a, 1976b, 1976c) for scale and rotation invariance. The realization of the Mellin transform is given by a logarithmic polar mapping of the input image followed by a Fourier transform.

Some studies have been done confirming the invariance to position, scale and rotation in the visual cortex in primates and humans (Schwartz, 1977, 1980, 1984) through a logarithmic polar mapping from the retina to the visual cortex as is known in the optical and digital pattern recognition. In this last aspect, for the majority of the digital systems the process is very different to the sensorial visual system, because to its natural complexity composition. The digital images are obtained in different environment conditions in an optical-digital sensor that causes several problems for the identification and characterization of the object using computerized vision systems, also the study is limited to static objects, and only bi-dimensional images are considered.

The scale transform has been proposed (Cohen, 1993, 1995) and is very suitable to scale sensitivities instead of the well known Mellin-Fourier transform. It has been applied to different areas such as image filtering and denoising (Cristóbal et al., 1998), in the identification and registration of some alphabetic letters and diatoms by computing the power cepstrum of the log-polar scale mapping (Pech-Pacheco et al., 2000) and in the automatic identification of phytoplanktonic algae (Pech-Pacheco et al., 2001) and in the analysis of letters scaled and rotated (Pech-Pacheco et al., 2003).

In this work, we obtain some results with a new computational algorithm for the recognition of several objects, independently of its size, angular orientation, displacement and noise. We use the scale transform and the k -th law nonlinear filter (Vijaya Kumar & Hassebrook, 1990) with a nonlinearity strength factor of $k=0.3$ (Coronel-Beltrán & Álvarez-Borrego, 2008). A k th

law nonlinear filter is introduced to realize the digital invariant correlation that gives us information on the similarity between different objects. The nonlinear strength factor is the exponent in the modulus of the Fourier transform of the object to be recognized in the expression of the nonlinear filter. This kind of filter has advantages compared with the phase only filter (POF) (Horner & Gianino, 1984) and other linear filters, due to its great capacity to discriminate objects, the maximum value of the correlation peak is well localized, narrow, with small sidelobes and the output plane is less noisy. In other works, a k th law joint transform correlator is used (Javidi, 1989a, 1989b, 1990), instead of a k th law nonlinear filter, in an optical coherent system (Javidi, 1989c), with better results, where the nonlinear characteristics are used to generate the nonlinear filter with an electrically addressed Spatial Light Modulator (SLM) located in the Fourier plane of the optical correlator. It is shown that both types of nonlinear filter produce better correlation performance compared with linear filters (Javidi, 1990). In our case, we used the k th law nonlinear filter because we are treating an invariant digital system and not an optical system. However, in an optical system it is difficult to implement the scale transform in order to have the invariances to scale and rotation.

In this work, the nonlinearity affects the Fourier magnitude of both the input signal and the reference signal. We applied this method for the recognition of the alphabetic letters in Arial font type and plain style with one rotational degree and one percent increments for rotation and scaling, respectively, until a complete rotation of 360 deg and $\pm 25\%$ scale variation is achieved. When the input scene is in presence of additive Gaussian and impulse salt-and-pepper (S&PP) noise we analyzed the performance of the nonlinear filter using the discrimination capability (DC) metric. The results were improved significantly when we introduced in the correlation digital system the nonlinear Spearman correlation.

The material of this work is organized as follows: in section 2, the preliminary concepts used to construct the invariant digital system are introduced. In section 3, the performance metrics used to evaluate the filters in the correlation output plane are presented. In section 4, the nonlinear invariant correlation method is described. Section 5 shows the results of some examples using the digital invariant correlation system with a nonlinear filter. Moreover, the results obtained by this new methodology were compared using the nonlinear and phase only filters. In section 6, a target immersed in Gaussian and S&PP noise is treated and the discrimination coefficients are shown. In section 7, the digital invariant system with a nonlinear filter in conjunction with a nonparametric statistical method is presented. In section 8, a comparative analysis of different font types in plain and italic style letters and the effects of five foreground/ background color combinations using an invariant digital correlation system with a nonlinear filter is given, and in section 9 the conclusions of our digital system for nonlinear invariant correlation are given.

2. Preliminary concepts

In this section, we provide a brief background of the principal concepts used in this work. These are: the nonlinear correlation filter, the phase only filter and the scale transform. In the first, the k -th law is implicit in this kind of filter. In the second, we show that this filter is a consequence of the most general filter defined as the nonlinear filter with $k=0$. And for the last, we have the scale transform as a special case of the Mellin transform that form a family of Mellin transforms depending of a real fixed parameter.

2.1 The k -th law nonlinear filter

A nonlinear correlation filter denoted by H_{NLF} is expressed as (Vijaya Kumar & Hassebrook, 1990)

$$H_{NLF}(u, v) = |S(u, v)|^k \exp[-j\phi(u, v)], \quad 0 < k < 1 \quad (1)$$

where $|S(u, v)|$ is the modulus of the Fourier transform of the object to be recognized, $j = \sqrt{-1}$, k is the nonlinearity strength factor and $\phi(u, v)$ is the phase of the filter's Fourier transform. We can manipulate the discrimination capabilities of the nonlinear correlator system by varying the k value between 0 and 1 to determine the best k value for the nonlinear filter.

2.2 The phase only filter

From equation (1), taking $k=0$, we have the phase only filter that is denoted as (Horner & Gianino, 1984)

$$POF = \exp[-j\phi(u, v)]. \quad (2)$$

2.3 The scale transform

The scale transform is a special case of the Mellin transform, where the last is defined as (De Sena & Rocchesso, 2007)

$$M_f(p) = \int_0^\infty f(x) x^{p-1} dx, \quad (3)$$

in the complex variable $p = -jc + \beta$, with the fixed parameter $\beta \in \mathbb{R}$ and the independent variable $c \in \mathbb{R}$. This family of transforms is called the β -Mellin transform. The real part of the complex variable p is parameterized, for the case $\beta = 1/2$ we have the scale transform. Other values for β are possible, for $\beta = 0$ we have the compression/ expansion invariant transform, and for $\beta = -1$ we have the form invariant transform. Therefore, the scale transform is a restriction of the Mellin transform on the vertical line $p = -jc + 1/2$.

We introduce the scale transform due to its property of invariance to size changes. The scale transform and its inverse are given in one-dimension by (De Sena & Rocchesso, 2004)

$$D_f(c) = (2\pi)^{-1/2} \int_0^\infty f(x) \exp[-(jc - 1/2) \ln x] dx, \quad (4)$$

and

$$f(x) = (2\pi)^{-1/2} \int_{-\infty}^\infty D_f(c) \exp[(jc - 1/2) \ln x] dc. \quad (5)$$

We used the 2-D scale transform in polar coordinates (r, θ) with the log of the radial coordinate $\lambda = \ln r$, that is expressed as (Cristóbal et al., 1998)

$$D(c_\lambda, c_\theta) = (2\pi)^{-1/2} \int_0^\infty \int_0^{2\pi} \exp(\lambda/2) f(\lambda, \theta) \exp[-j(\lambda c_\lambda + \theta c_\theta)] d\lambda d\theta, \quad (6)$$

where the non-separable scale transform implementation has been utilized in order to maintain the invariance to rotation (Pech-Pacheco et al., 2003).

3. Metrics used in performance evaluation

In this section, we present two well-known metrics used to evaluate the performance of the filters in the correlation output plane. These are: the peak-to-correlation energy and the discrimination capability metrics. The first is used for objects free of noise and the second for objects immersed in noise.

3.1 The peak-to-correlation energy (PCE)

The peak-to-correlation energy PCE performance metric is defined as (Javidi & Horner, 1994)

$$PCE = \frac{|E\{c(0,0)\}|^2}{E\{|c(x,y)|^2\}}, \quad (7)$$

where the numerator is the correlation peak intensity expected value and the denominator is the mean energy expected value in the correlation plane.

3.2 The discrimination capability (DC)

If we consider that an object is embedded in a noise background, the discrimination coefficient that is a modified version of the discrimination ratio (Vijaya & Hassebrook, 1990) is given by

$$DC = 1 - \frac{|C^N(0,0)|^2}{|C^{OBJ}(0,0)|^2}, \quad (8)$$

where the correlation peak produced by the object is C^{OBJ} , and the highest peak of just the noise background is C^N .

4. The nonlinear invariant correlation method

In this section we present the methodology used in this work of the digital invariant correlation system with a nonlinear filter. First, we describe in each step the process to obtain the nonlinear filter of the target. Secondly, the invariant correlation system with the nonlinear filter is described. In both cases, the algorithms are represented with simplified block diagrams.

4.1 Obtaining the digital invariant system with a nonlinear filter (DISNF)

The steps to obtain the DISNF are showed in Fig. 1. In step (1), we have the original image, $f(x, y)$ consisting of the target. The fast Fourier transform (FFT) is calculated in step (2). The modulus of the Fourier transform denoted as $|F(u, v)|$, is obtained in step (3); in this way the displacement of the input image is not affected in the Fourier plane according to the well known shift theorem (Goodman, 2005). Next, we applied a parabolic filter (step 4) (Pech-Pacheco et al., 2003). This type of filter attenuates low frequencies and passes high frequencies that increases the sharpness in the details of the object.

The next step is to introduce the scale factor given by $r^{1/2}$ (step 5) (r is the radial spatial frequency, the origin of which lies at zero frequency in the optical representation of the

Fourier spectrum). This process is what differentiates the scale transform from the Mellin transform.

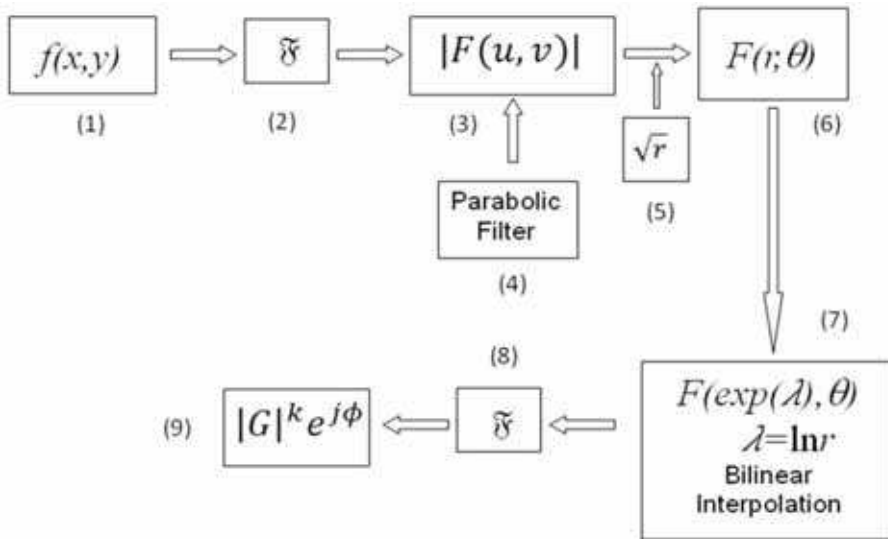


Fig. 1. Simplified block diagram for obtaining the nonlinear filter

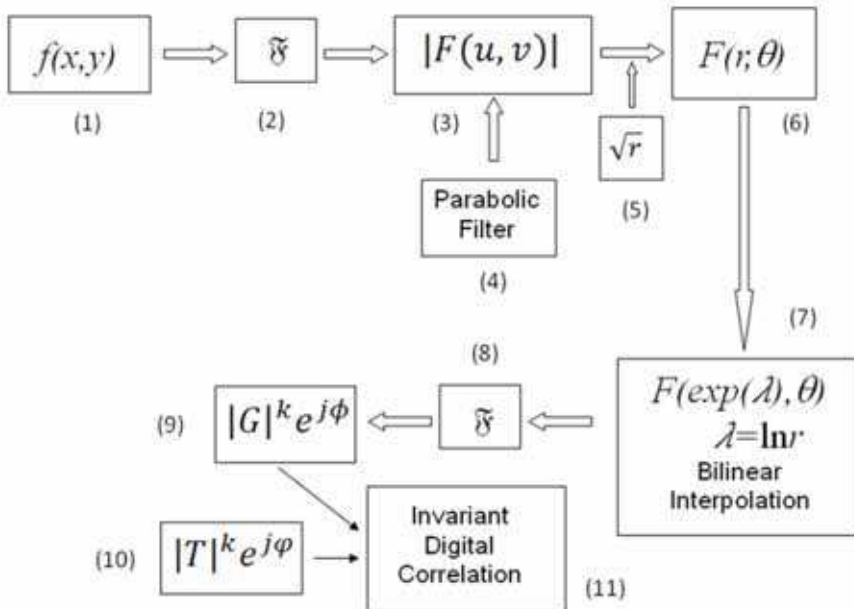


Fig. 2. Simplified block diagram representing the invariant correlation system with a nonlinear filter

Cartesian coordinates are mapped to polar coordinates to obtain the rotation invariance (step 6). In this step we introduced a bilinear interpolation of the first data of coordinate conversion. This is done to avoid the aliasing due to the log-polar sampling. A logarithmic scaling is made in the radial part in polar coordinates (step 7). And taking the FFT (step 8), we obtain a filter with invariance to position, rotation and scale (step 9). In this step we write the filter in a similar manner to equation (1), where $|T|$ and ϕ are the modulus and the phase of the Fourier transform of the object to be recognized, respectively, after to consider the invariance.

4.2 The nonlinear invariant correlation

The steps to realize the invariant correlation with a nonlinear filter are shown in Fig. 2. The problem image which contains or not the target is the input image (step 1). From the step (1) to (9), the procedure is the same as in Fig. 1. The step (9) shows the nonlinear information of the problem image, where $|G|$ and ϕ are the modulus and the phase of the Fourier transform of the problem image, respectively, after to consider the invariance. The steps (9) and (10) show the correlation procedure to obtain the invariant digital correlation (step 11) to position, rotation and scale using a nonlinear filter. The linear and nonlinear filter inside this invariant process is a combination more powerful to recognize different patterns with different scale and rotations.

5. Computer simulations

In this section, we present a numerical statistical experiment to find the best k nonlinearity strength factor value for the nonlinear filter. The results were box plotted, peak-to-correlation energy (PCE) *vs* k , one for the rotation and the other for the scale. Image **A** was used as the target (Fig. 3). Obtaining that the results for the maximum k value were the same as in (Coronel-Beltrán & Álvarez-Borrego, 2008), that is $k=0.3$.



Fig. 3. Images used for obtaining the best k value. Image **A** was used like the target

A box plot graph for the peak-to-correlation energy PCE vs the nonlinearities k values is shown in Fig. 4 for the rotation case, from $k=0$ to $k=1$ for the target **A** correlated with the 15 problem images denoted for **A, B, C, ... O**, shown in Fig. 3, rotated, with one rotation degree increment, from 0 to 179 rotation degrees. This graph shows the mean value with one standard error ($\pm SE$) and two standard errors ($\pm 2*SE$) for the PCE. The number of images processed for each k value was 2700. Because we select 11 different k values, 0, 0.1, 0.2, ..., 1.0, so we have a total of 29700 statistically processed images.

From Fig. 4, we observe that for values $0.1 \leq k \leq 0.4$ we have the best performance of the nonlinear filter.

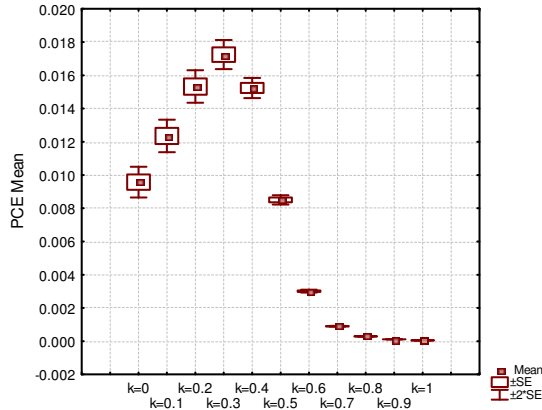


Fig. 4. Box plot graph for the peak-to-correlation energy PCE vs the nonlinearities k values, for the image **A** correlated with the 15 rotated problem images in Fig. 3

In a similar manner, a box plot graph for the peak-to-correlation energy PCE vs the nonlinearities k values is shown in Fig. 5 for the scale case, from $k=0$ to $k=1$ for the target **A**

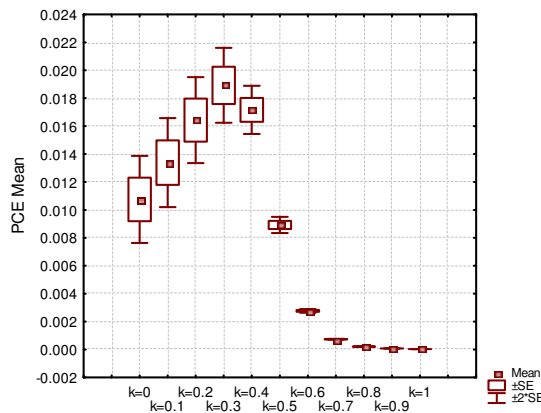


Fig. 5. Box Plot graph for the peak-to-correlation energy PCE vs the nonlinearities k values, for the image **A** correlated with the 15 scaled problem images in Fig. 3

correlated with the 15 problem images scaled, with one percent increment, from 75% to 125%. This graph shows the mean value with one standard error ($\pm 1 * SE$) and two standard errors ($\pm 2 * SE$) for the PCE. The number of images processed for each k value was 765. We have the same 11 different values of k used for the rotation problem, hence we have a total of 8415 statistically processed images.

From Fig. 5, we observe that for values $0.1 \leq k \leq 0.4$ we have the best performance of the nonlinear filter again.

For the rotated and scaled cases, the result for the best k value was the same, $k=0.3$.

5.1 DISNF applied to alphabetic letters

Some results obtained using a DISNF for testing this method for changes of rotation and scale of the letter **E** are presented. In other example the cross-correlations were calculated for a nonlinear and a phase only filters and its performance was compared.

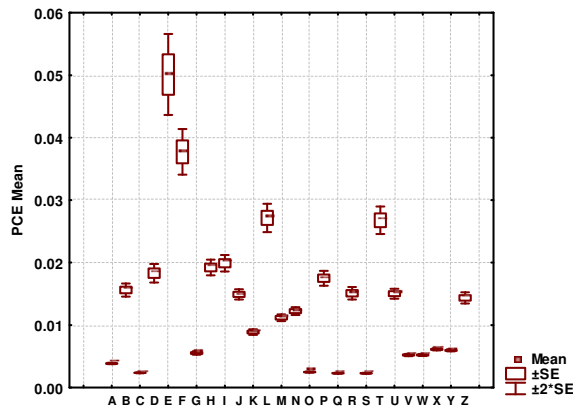


Fig. 6. Performance of the filter **E** for rotation

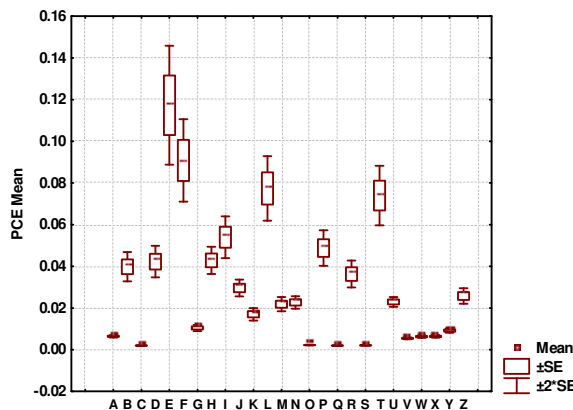


Fig. 7. Performance of the filter **E** for scale from 75% to 125%

We used the k strength factor value for the nonlinear filter using the letter **E** for rotation and scale, $k=0.3$. The results of the filter **E** for rotation and scale are shown in Figs. 6 and 7. The filter is correlated with each one of the 26 alphabet letter, with one rotation degree increment, from 0 to 359 deg and scaled from 75% to 125% with one percent increment considering that the filter is 100% in scale.

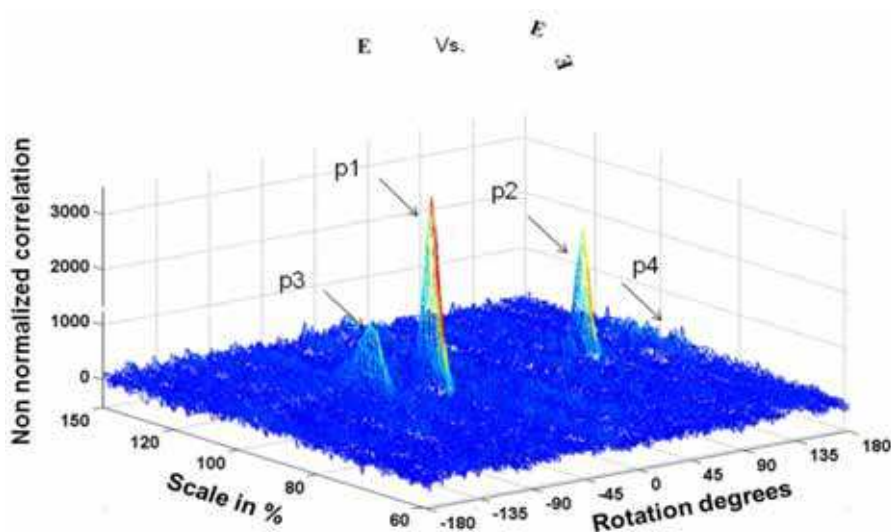
With respect to rotation the algorithm has a good performance to $\pm 2^*SE$ when we want to recognize the **E** letter (Fig. 6). More results were obtained using different characters like target (Coronel-Beltrán & Álvarez-Borrego, 2008). From Fig. 7 we observe an overlap of the letter **E** with the **F** and **L** letters, but, to $\pm 1^*SE$ the invariant correlation had a good performance.

5.2 Comparison of an invariant digital system using nonlinear and phase only filters

We present another correlation examples using a nonlinear filter with the same $k=0.3$, and compared with the phase only filter. Figs. 8 and 9 show the graphs of the output correlation performance of these filters where the filter and the problem image are the letters E. We observe a less noisy correlation plane (Fig. 8a) with peaks well defined p1, p2, and p3 when a nonlinear filter is used. The PCE value was 0.0215. An output plane correlation with more background noise is presented when in the invariant correlation a phase only filter is used (Fig. 8b). For this case the PCE value was 0.0057.

Because the images in the problem image have the same scale like the target we analyze in this example the rotation angles only. So, Fig. 8c shows one transect in the rotation axis of the Fig. 8a. We can observe three peaks, p1, p2 and p3 and a small peak p4.

So, in Fig. 8c, the peaks are along the rotation axes that correspond to each letter E rotated in the problem image.



(a)

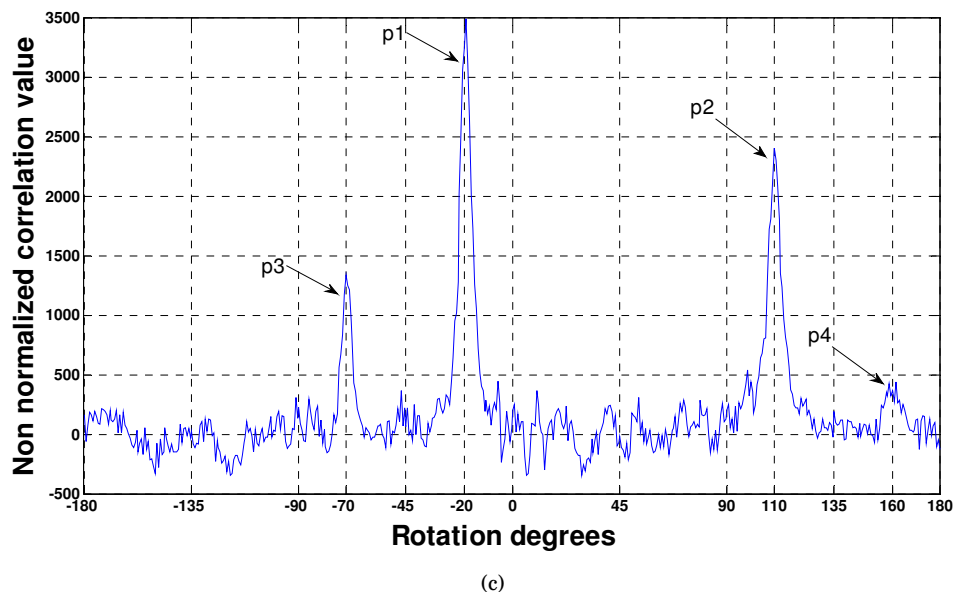
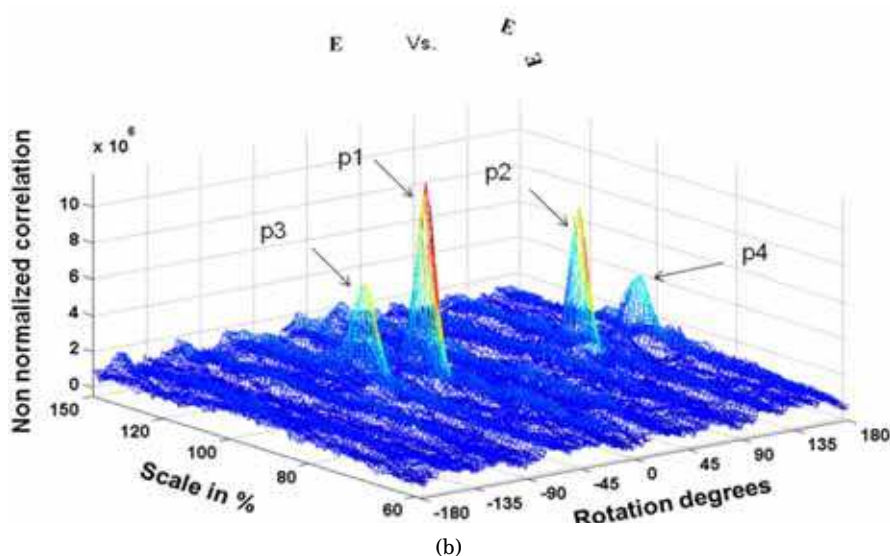


Fig. 8. Invariant correlation to rotation using (a) a nonlinear filter with $k=0.3$ and $PCE=0.0215$, (b) a phase only filter with $PCE=0.0057$, and (c) a rotation transect of (a)

In the image problem of Fig. 8a we have two E letters, one is rotated -20 deg and the other to 110 deg. The peak p1 corresponds to -20 deg, the peak p2 corresponds to 110 deg, the peak p3 to -70 deg and the peak p4 corresponds to 160 deg. Peaks p1 and p4, and peaks p2 and p3

are complementary angles, because when we rotate an object to certain angle, there is another angle for the same object (Fig. 8c). So, in correlation values $p1+p4=p2+p3$.

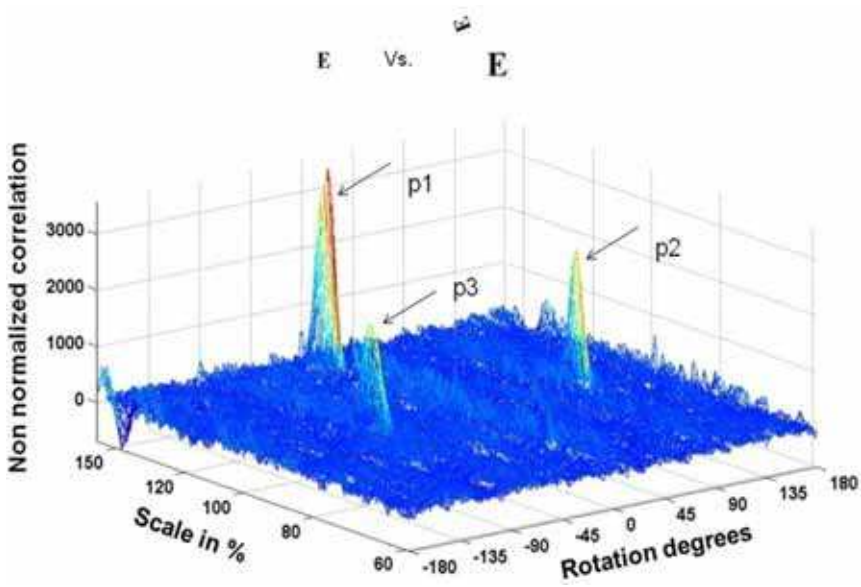
In Fig. 8b we have the appearance of peak p4. This peak corresponds to 160 deg that is complementary to -20 deg of the peak p1. So, $p1+p4=p2+p3$ again.

In the image problem of Fig. 9 we have two E letters; one is rotated 110 deg and the other to zero deg and scaled to 150% with respect to the filter. The peak p1 corresponds to zero deg. The peak p2 corresponds to 110 deg and its correspondent peak p3 to -70 deg.

We can observe from these figures that when the rotation angle of the character is small the secondary peak tends to be smaller.

Figs. 9a and 9b show the output correlation plane when we have in the problem image one character with different rotation and scale and we are using a nonlinear and a linear filter respectively in order to make the recognition of the letter. However, one transect along the scale axis is shown in Fig. 9c. The peak p1 is observed exactly in the 150% value in the scale axis.

Because we are studying the behavior of the nonlinear versus the linear filter a quantitative comparison between these filters were done using the PCE metric. A desirable attribute of a correlator is capable of producing sharp correlation peaks. This characterization is taken account by the PCE. Considering a nonlinear filter compared with the phase only, the first one concentrates most of the energy that passes through the filter in the correlation peak. We denote PCE_{NLF} , PCE_{POF} the PCE values for the nonlinear filter and the phase only filter, respectively. In this manner, the ratios of these filters were, from Fig. 8: $PCE_{NLF}/PCE_{POF}=3.77$; and from Fig. 9: $PCE_{NL}/PCE_{POF}=4.1$. In all these cases, the PCE value for the nonlinear filter was better compared with the phase only filter.



(a)

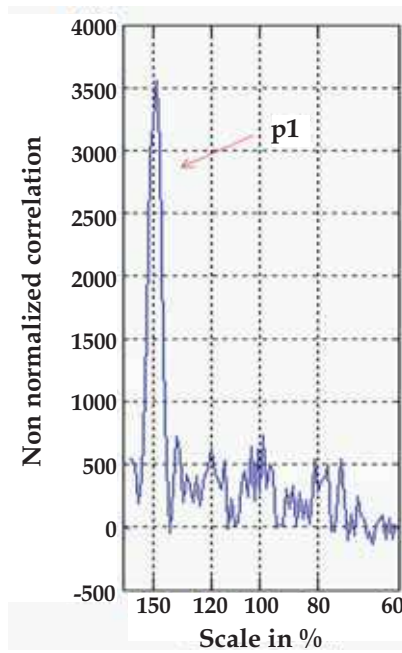
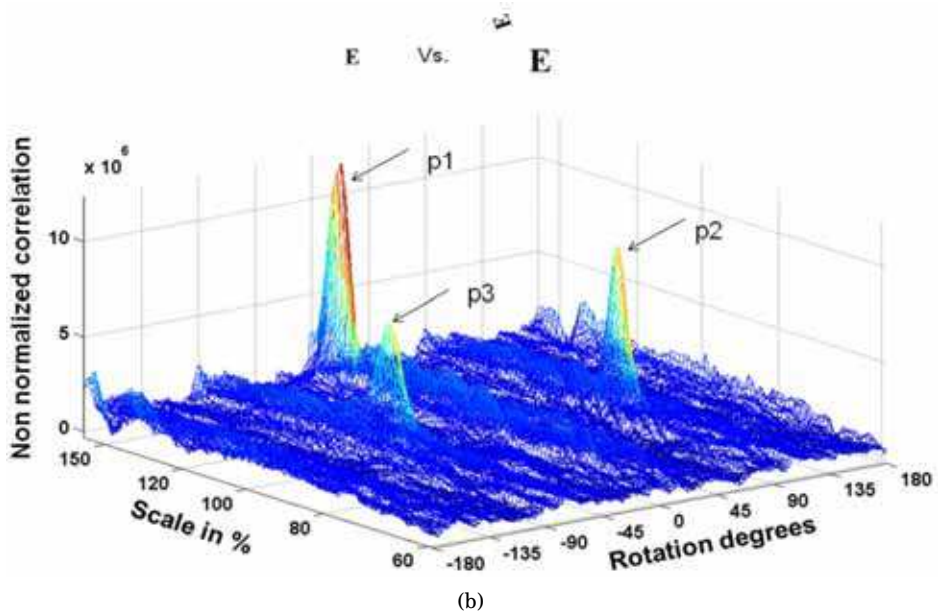


Fig. 9. Rotation and scale invariant correlation using (a) nonlinear filter with $k=0.3$ and $PCE=0.025$, (b) a phase only filter with $PCE=0.0061$, and (c) a scale transect of (a)

6. Target with noise

In this section we treat with two kinds of noise applied to the target. One is the additive Gaussian noise and the other is the S&PP noise (Fig. 10).

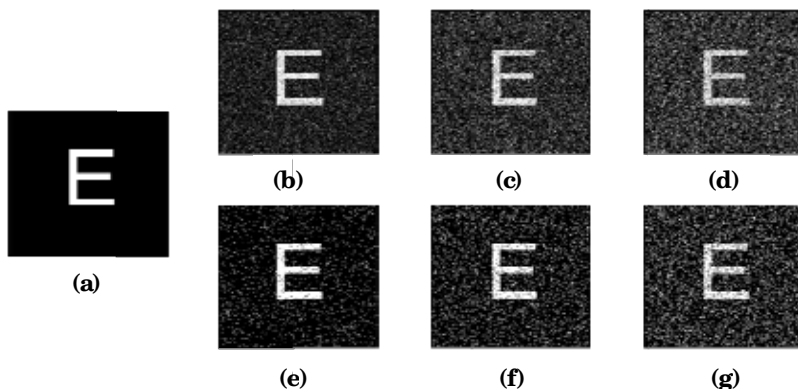


Fig. 10. Target free of noise (a), with additive Gaussian noise of mean zero and variance of 0.1 (b), 0.2 (c) and 0.3 (d), and with S&PP noise of noise density of 0.1 (e), 0.2 (f) and 0.3 (g)

Figs. 11 and 12 show the graphs of the discrimination coefficient using 30 numerical experiments to a 95% level of confidence for a nonlinear filter with $k=0.3$ when an additive Gaussian noise, with mean zero, and a S&PP noise are considered. In both graphs we have the DC mean *vs.* the variance and the density noise. From these graphs we observe that the filter can recognize the object with a noise variance of approximately 0.27 and a noise density of approximately 0.3 for additive Gaussian and S&PP noise, respectively.

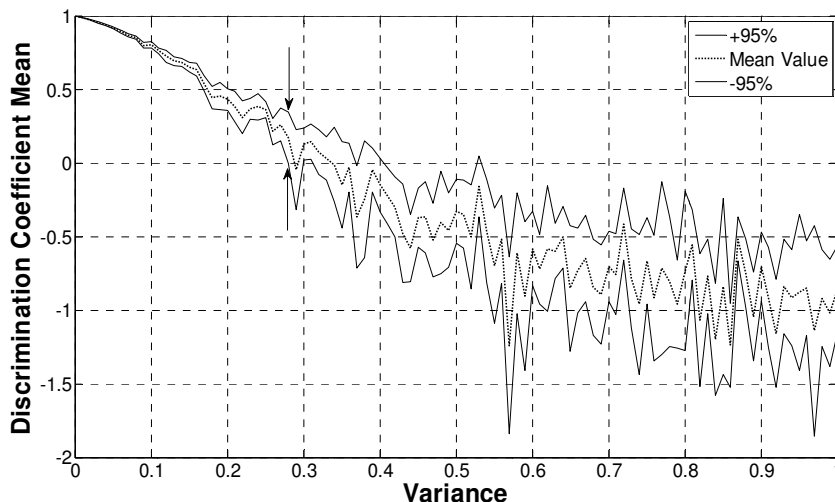


Fig. 11. Performance of a nonlinear filter with $k=0.3$ in the presence of additive Gaussian noise

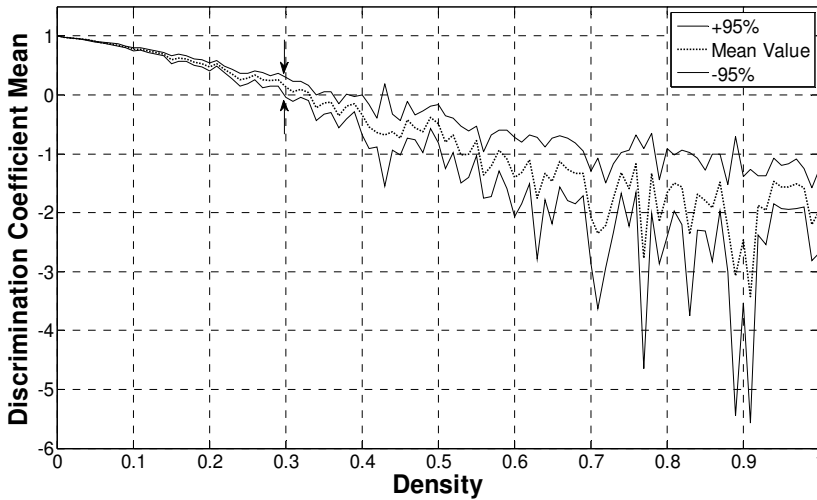


Fig. 12. Performance of a nonlinear filter with $k=0.3$ in the presence of S&PP noise

It is important to say that the maximum value that can be obtained with the DC is unity, while values below zero indicate that the filter does not recognize the object.

7. DISNF and the Spearman correlation

To study the improvement of the method when the images are embedded in an additive Gaussian noise and in one S&PP noise, we used a nonparametric method, called the rank statistics, to calculate correlation between two images. Substituting the value of each pixel for its corresponding rank, in the normalized correlation expression, a nonlinear correlation expression is obtained [Spearman’s rank correlation (SRC)]. Taking this into consideration, the 2-D SRC can be expressed as (Guerrero-Moreno & Álvarez-Borrego, 2009)

$$R(k, l) = 1 - \frac{6 \sum_{m,n \in W} (r_t(m,n) - r_s(m+k,n+l))^2}{|W| \cdot (|W|^2 - 1)}, \tag{9}$$

where $\{r_t(m,n), m = 1,2,\dots,N; n = 1,2,\dots,M\}$ is the rank of the target, $\{r_s(m+k,n+l), k = 1,2,\dots,N; l = 1,2,\dots,M\}$ is the rank of the problem image, W is the size of each image, R is the Spearman rank correlation and m, n, k, l are the spatial coordinates.

Fig. 13 shows a block diagram representing the SRC in conjunction with the nonlinear method (SDISNF) in order to increase the tolerance to the noise. In this figure, from the step (1) to the step (10), the procedure is the same as in Fig. 2, except that now, step (11), we realize the inverse FFT for the steps (9) and (10). The step (12) is the SRC in the spatial domain and the step (13) give us the output correlation plane.

From Figs. 14 and 15 we observe the improvement of the filter performance when an additive Gaussian noise, with mean zero, and S&PP noise is added respectively. From these graphs we observe that the filter can support a noise variance of approximately 0.92 and a noise density of approximately 0.54 for additive Gaussian and S&PP noise, respectively.

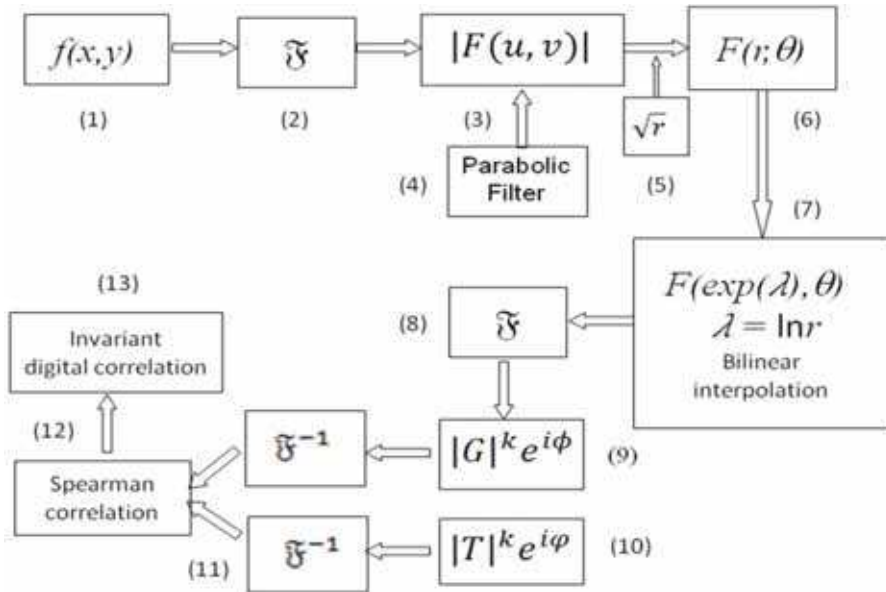


Fig. 13. Simplified block diagram representing the invariant correlation system with a nonlinear filter using the SDISNF

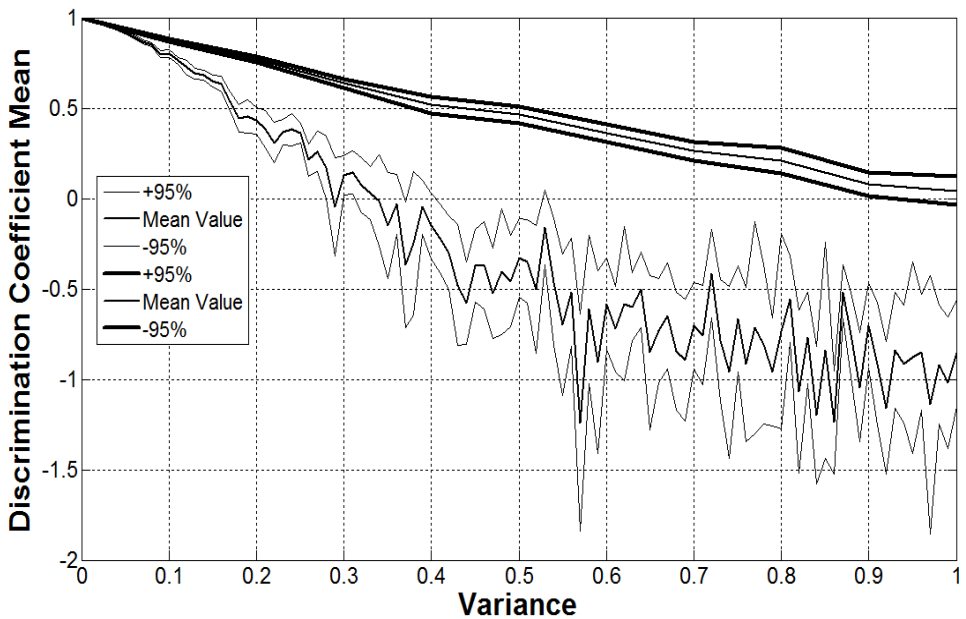


Fig. 14. Performance comparison with SDISNF when the target is embedded in additive Gaussian noise

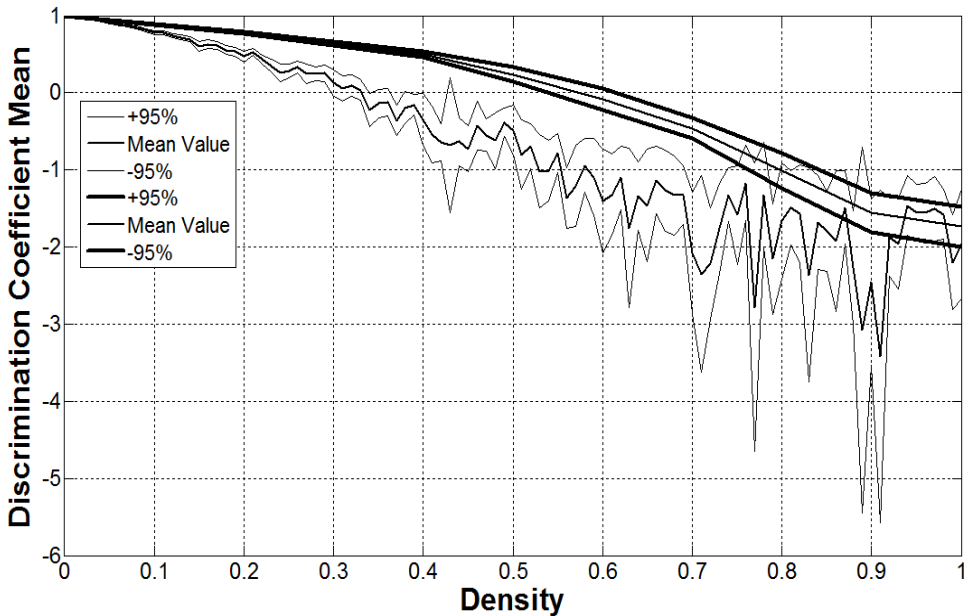


Fig. 15. Performance comparison with SDISNF when the target is immersed in S&PP noise

These figures show the performance comparison when we used the SDISNF for the target immersed in additive Gaussian and S&PP noise. From these figures we can see that the discrimination coefficient is greater than for the only the additive Gaussian noise by a factor of three and for S&PP noise the factor is approximately two.

8. Comparative analysis between different font types and styles letters using a nonlinear invariant digital correlation

In this section we present a comparative analysis of the letters in Times New Roman (TNR), Courier New (CN) and Arial (Ar) font types in Plain & Italicized style and the effects of 5 foreground/ background color combinations using an invariant digital correlation system with a nonlinear filter with $k=0.3$ (Coronel-Beltrán & Álvarez-Borrego, 2010). The evaluation of the output plane with this filter is given by the peak-to-correlation energy (PCE) metric. The results show that the letters in TNR font have a better mean PCE value when is compared with the CN and Ar fonts. This result is in agreement with some studies (Hill, 1997) about text legibility and for readability where the reaction time (RT) of some participant individuals reading a text is measured. We conclude that the PCE metric is proportional to $1/RT$.

Fig. 16 shows the mean PCE values obtained versus the letters in Arial (Ar), Courier New (CN) and Times New Roman (TNR) font types in Italicized and Plain style with 5 foreground/ background color combinations; black-on-white (BK/ W), green-on-yellow (GN/ Y), red-on-green (R/ GN), white-on-blue (W/ BL) and yellow-on-blue (Y/ BL), using an invariant digital correlation system with a nonlinear filter with $k=0.3$. The

foreground/ background colors were selected with color coordinates RGB(r,g,b), normalized to [0-255](bytes), as follows; red: (255,0,0), green: (0,128,0), blue: (0,0,255), yellow: (255,255,0), black: (0,0,0) and white: (255,255,255). The letters are 512x512 pixels in size and bitmap file format with 256 colors. The results show that the letters in TNR font have a better mean PCE when is compared with the Ar and CN fonts.

For the italicized style we can observe from this graph that TNR font had a greater mean PCE value compared with Ar and CN fonts. All of them in this style had the same performance and the color combinations were irrelevant.

For the plain style we can observe that TNR font had also a greater mean PCE value compared with Ar and CN fonts. But contrary to the italicized style, in the plain style we have found that the color combinations affect the mean PCE value of the font type letters. The black-on-white and the white-on-blue color combinations had the higher mean PCE values. For the green-on-yellow, red-on-green and yellow-on-blue color combinations, there were no significant changes in the mean PCE values, and like in the italicized case, their behaviour was the same, and the color combinations were irrelevant as well as their mean PCE was statistically not significant.

Using the RT of some participant individuals, reading a text, the effects of six color combinations, three font types (Arial, Courier New & Times New Roman) in Italicized and Plain styles were studied (Hill, 1997) and the results showed that for green-on-yellow, in italicized style, the TNR font had best RT values than Arial font. For all color combinations in italicized and plain style, the TNR font has RT smaller than the Ar font, except for black-on-white and red-on-green in italicized style, and for black-on-white and white-on-blue in plain style.

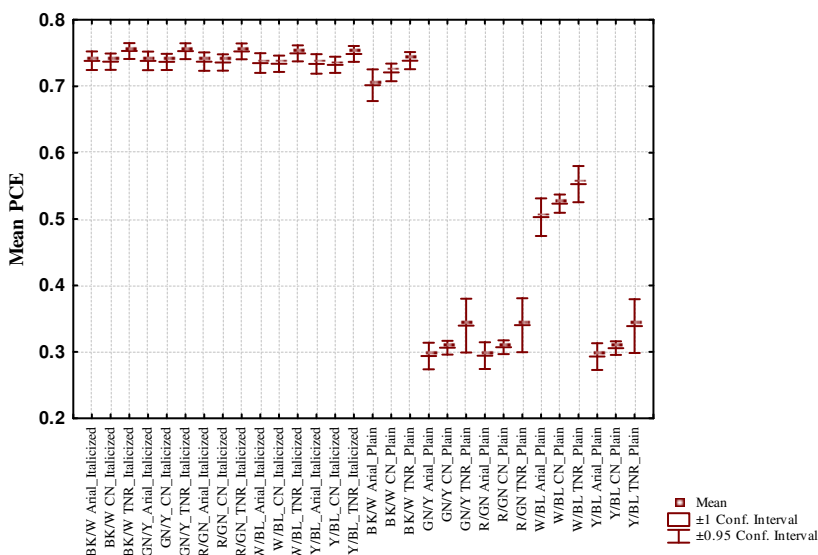


Fig. 16. Performance of the letters Arial (Ar), Courier New (CN) and Times New Roman (TNR) with font types in Italicized & Plain style and 5 foreground/ background color combinations

This algorithm was compared with respect to the one published by Alvarez-Borrego & Castro-Longoria (2003), both similar in their use for pattern recognition. Our new algorithm has a computing time that is 20% less. To perform the simulations, a computer, Dell PS_420 with Intel (R) Core (TM) 2 Quad CPU Q6700 @ 2.66 GHz processor, 2.00 GB of RAM, was used.

9. Conclusion

A digital system for invariant correlation using a nonlinear filter was tested with the maximum nonlinearity strength factor value $k=0.3$ that was determined experimentally for both scale and rotation. We used the alphabet letters in Arial font type where each one of these letters was taken as a target and correlated with each one for the other letters and showed that our system worked efficiently for the discrimination objects. This nonlinear invariance correlation method was applied using nonlinear and only phase filters for different objects scaled and rotated, Times New Roman font type E letter, and we found a better PCE performance for the nonlinear filters. The DC performance of the noisy target, for additive Gaussian noise and impulse salt-and-pepper noise, was improved significantly applying the SDISNF.

This new combination (SDISNF) is so more powerful than other methods when images with noise are analyzed.

In addition, we presented an analytical method, using a digital invariant correlation, for comparison and to analyze different font and style letters with five color combinations. Our results showed a better output for the TNR in comparison with the Ar font letters in italicized & plain style. And generally, italicized letter style had greater PCE values than plain style letter. These results were in accord to some other studies realized with subjective methods. Our results can be useful for studying the effects of background color combinations on legibility displayed on a computer screen from the Web, email, or other texts written in books, newspapers, magazines, etc., and its improvement as well as in readability. We conclude that the PCE metric is proportional to $1/RT$. It would be interesting investigate the relationship between our method based in analytical mathematical functions and those other subjective empirical methods used by psychologists and Web designers, among others.

10. Acknowledgment

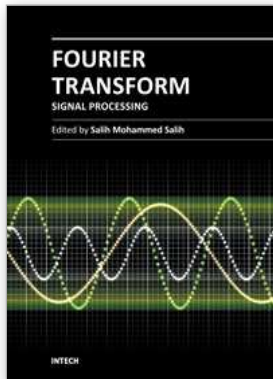
This work was partially supported by the grant 102007 from CONACYT and a grant from Universidad de Sonora.

11. References

- Álvarez-Borrego, J & Castro-Longoria, E. Discrimination between *Acartia* (Copepoda: Calanoida) species using their diffraction pattern in a position, rotation invariant digital correlation. *J Plankton Res.*, Vol. 25, No. 2, pp. 229-233, ISSN 0142-7873
- Casasent, D. & Psaltis, D. (1976a). Scale invariant optical correlation using Mellin transforms. *Opt. Commun.*, Vol. 17, No. 1, April 1976, pp. 59-63, ISSN 0030-4018

- Casasent, D. & Psaltis, D. (1976b). Scale invariant optical transform. *Opt. Eng.*, Vol. 15, No. 3, pp. 258-261, May-June 1976, ISSN 0091-3286
- Casasent, D. & Psaltis, D. (1976c). Position, rotation, and scale invariant optical correlation. *Appl. Opt.*, Vol. 15, No. 7, July 1, pp. 1795-1799, ISSN 0003-6935
- Cohen, L. (1993). The scale representation. *IEEE-SP*, Vol. 41, No. 12, Dec. 1993, pp. 3275-3292, ISSN 1053-587X
- Cohen, L. (1995). *Time Frequency Analysis* (A.V. Oppenheim), Prentice Hall, ISBN-10 0135945321, New Jersey
- Coronel-Beltrán, A. & Álvarez-Borrego, J. (2008). Nonlinear filter for pattern recognition using the scale transform, *Proc. SPIE*, Vol. 7073, 70732H, San Diego, California, USA, August 2008
- Coronel-Beltrán, A. & Álvarez-Borrego, J. (2010). Comparative analysis between different font types and letter styles using a nonlinear invariant digital correlation. *J Mod Optics*, Vol. 57, No. 1, (January 2010), pp. 58-64, ISSN 0950-0340 print/ ISSN 1362-3044 online
- Cristóbal, G.; Cuesta, J & Cohen, L. (1998). Image filtering and denoising through the scale transform, *Proc. IEEE-SP, International Symposium on Time-Frequency and Time-Scale Analysis*, ISBN 0-7803-5073-1, pp. 617-620, Pittsburgh, PA, USA, October 1998
- De Sena, A. & Rocchesso, D. (2004). A fast Mellin transform with applications in DAFx, *Proceedings of the 7th International Conference on Digital Audio Effects (DAFx'04)*, Naples, Italy, October 2004, pp. 65-69
- De Sena, A. & Rocchesso, D. (2007). A Fast Mellin and Scale Transform. *EURASIP Journal on Advances in Signal Processing*, Vol. 2007, pp. 1-9
- Goodman, J.W. (2005). *Introduction to Fourier Optics*, Roberts & Company, ISBN 0-9747077-2-4, Greenwood Village, CO, USA, pp. 435-436
- Guerrero-Moreno, R. & Álvarez-Borrego, J. (2009). Nonlinear composite filter performance. *Opt. Eng.* Vol. 48, No. 6, 067201, June 2009, ISSN 0091-3286
- Hill, A.L. (1997). Readability of websites with various foreground/ background color combinations, font types and word styles. Stephen F. Austin State University. <http://www.laurenscharff.com/research/AHNCUR.html>
- Horner, J.L. & Gianino, P.D. (1984). Phase-only matched filtering. *Appl. Opt.* Vol. 23, No. 6, March 15, pp. 812-816, ISSN 0003-6935
- Javidi, B. (1989a). Nonlinear joint power spectrum based optical correlation. *Appl. Opt.* Vol. 28, No. 12, June 15, pp. 2358-2367, ISSN 0003-6935
- Javidi, B. (1989b). Synthetic discriminant function-based binary nonlinear optical correlator. *Appl. Opt.* Vol. 28, No. 13, July 1, pp. 2490-2493, ISSN 0003-6935
- Javidi, B. (1989c). Nonlinear matched filter based optical correlation. *Appl. Opt.* Vol. 28, No. 21, November 1, pp. 4518-4520, ISSN 0003-6935
- Javidi, B. (1990). Comparison on nonlinear joint transform correlator and nonlinear matched filter based correlator. *Opt. Commun.* Vol. 75, No. 1, 1 February 1990, pp. 8-13, ISSN 0030-4018
- Javidi, B. & Horner, J.L. (1994). *Real-Time Optical Information Processing*, Academic Press, Boston, ISBN 0123811805
- Pech-Pacheco, J.L.; Cristóbal, G., Álvarez-Borrego, J & Cohen, L. (2000). Power cepstral image analysis through the scale transform, *Proc. SPIE*, Vol. 4113, pp. 68-79

- Pech-Pacheco, J.L.; Cristóbal, G., Álvarez-Borrego, J & Cohen, L. (2001). Automatic system for phytoplanktonic algae identification. *Limnetica*, Vol. 20(1), pp. 143-157, ISSN 0213-8409
- Pech-Pacheco, J.L.; Álvarez-Borrego, J, Cristóbal, G. & Mathias, S.K. (2003). Automatic object identification irrespective to geometric changes. *Opt. Eng.*, Vol. 42, No. 2, February 2003, pp. 551-559, ISSN 0091-3286
- Schwartz, E.L. (1977). Afferent Geometry in the Primate Visual Cortex and the Generation of Neuronal Trigger Features. *Biol. Cybernetics*, Vol. 28, No. 1, pp. 1-14, ISSN 0340-1200
- Schwartz, E.L. (1980). Computational anatomy and functional architecture of striate cortex: A spatial mapping approach to perceptual coding. *Vision Res.*, Vol. 20, No. 8, Aug. 1980, pp. 645-669, ISSN 0042-6989
- Schwartz, E.L.; Christman, D. R. & Wolf, A.P. (1984). Human primary visual cortex topography imaged via positron tomography. *Brain Res.*, Vol. 294, No. 2, Mar. 1984, pp. 225-230, ISSN 00068993
- Vander Lugt, A.B. (1964). Signal detection by complex spatial filtering. *IEEE Trans. Inf. Theory*, Vol. 10, No. 2, Apr. 1964, pp. 139-145, ISSN 0018-9448
- Vijaya Kumar, B.V.K. & Hassebrook, L. (1990). Performance measures for correlation filters. *Appl. Opt.*, Vol. 29, No. 20, July 10, pp. 2997-3006, ISSN 0003-6935



Fourier Transform - Signal Processing

Edited by Dr Salih Salih

ISBN 978-953-51-0453-7

Hard cover, 354 pages

Publisher InTech

Published online 11, April, 2012

Published in print edition April, 2012

The field of signal processing has seen explosive growth during the past decades; almost all textbooks on signal processing have a section devoted to the Fourier transform theory. For this reason, this book focuses on the Fourier transform applications in signal processing techniques. The book chapters are related to DFT, FFT, OFDM, estimation techniques and the image processing techniques. It is hoped that this book will provide the background, references and the incentive to encourage further research and results in this area as well as provide tools for practical applications. It provides an applications-oriented to signal processing written primarily for electrical engineers, communication engineers, signal processing engineers, mathematicians and graduate students will also find it useful as a reference for their research activities.

How to reference

In order to correctly reference this scholarly work, feel free to copy and paste the following:

Angel Coronel-Beltran and Josue Alvarez-Borrego (2012). Invariant Nonlinear Correlations via Fourier Transform, Fourier Transform - Signal Processing, Dr Salih Salih (Ed.), ISBN: 978-953-51-0453-7, InTech, Available from: <http://www.intechopen.com/books/fourier-transform-signal-processing/invariant-nonlinear-correlations-via-fourier-transform>

INTECH
open science | open minds

InTech Europe

University Campus STeP Ri
Slavka Krautzeka 83/A
51000 Rijeka, Croatia
Phone: +385 (51) 770 447
Fax: +385 (51) 686 166
www.intechopen.com

InTech China

Unit 405, Office Block, Hotel Equatorial Shanghai
No.65, Yan An Road (West), Shanghai, 200040, China
中国上海市延安西路65号上海国际贵都大饭店办公楼405单元
Phone: +86-21-62489820
Fax: +86-21-62489821

© 2012 The Author(s). Licensee IntechOpen. This is an open access article distributed under the terms of the [Creative Commons Attribution 3.0 License](#), which permits unrestricted use, distribution, and reproduction in any medium, provided the original work is properly cited.